Available online at www.sciencedirect.com
SCIENCE DIRECT®
Journal of Solid State Chemistry 177 (2004) 1188–1196
JOURNAL OF SOLID STATE CHEMISTRY
http://elsevier.com/locate/jssc

# TEM study of cation-deficient-perovskite related $A_nB_{n-1}O_{3n}$ compounds: the twin-shift option

G. Trolliard,[1] N. Ténèze, Ph. Boullay, and D. Mercurio*

*Science des Procédés Céramiques et de Traitements de Surface, UMR-CNRS 6638, Faculté des Sciences et Techniques, 123 avenue Albert Thomas, 87060 Limoges Cedex, France*

Received 31 July 2003; received in revised form 22 October 2003; accepted 26 October 2003

**Abstract**

Among hexagonal perovskites, the *B*-cation deficient perovskite-related compounds $A_nB_{n-1}O_{3n}$ present two kinds of structural types depending on the stacking sequences of their $AO_3$ layers. All these structures derive from the perovskite, which is periodically disturbed by planar defects. The structures with $(hhc\ldots c)$-type sequences, present successive perovskite blocks shifted from one another by a $1/3\langle 01\bar{1}0\rangle_H$ vector, while $(hc\ldots c)$-type sequences show twin plane boundaries. The non-stoichiometry of these compounds is in all cases closely associated with the distribution of these planar defects: shift planes or twin boundaries. In the hexagonal perovskites of the $A_nB_{n-1}O_{3n}$ series belonging to the $Ba_5Nb_4O_{15}$–$BaTiO_3$ system, the twin type structures is favored by high values of $n$ (number of octahedra layers within a perovskite blocks) and $t$ (Goldschmidt tolerance factor). The stability of the "shift" type structure surely comes from the preservation of a bcc cationic sub-lattice. However, this structural type results in the occurrence of a long-range order of vacant octahedra layers. The stability of the "twin" type structure is related to the drastic decrease of the periodicity of vacancies along the *c*-axis (every $n/2$ octahedra layers) but needs a very expanded three dimensional $BO_6$ octahedra sub-lattice (high value of $t$) and a specific order of the *B*-cations in the vicinity of the twin planes.


*Keywords:* Cation deficient perovskite; Planar faults; Electron diffraction; TEM

## 1. Introduction

The structure of perovskites $ABO_3$ can be described as the stacking of close packed $AO_3$ layers in a cubic sequence $(ABC,\ldots)$. The *B*-site cations occupy 1/4 of the octahedral cavities existing between the $AO_3$ layers in such a way that the $BO_6$ octahedra form a 3D network of corner sharing octahedra (CSO). Among the perovskite-related structures, the so-called "hexagonal" perovskites of the series $A_nB_{n-1}O_{3n}$ exhibit a structure also characterized by a close packing of $AO_3$ layers but differ from the "classical" cubic stacking of the perovskite by the introduction of hexagonal stacking sequence $(AB,\ldots)$. Hence, the name of "hexagonal" perovskite is actually used to describe mixed hexagonal-cubic $AO_3$ stacking sequences. These sequences can be advantageously described using the Jagodzinski notation [1,2] where a layer in the sequence is denoted *h* or *c* whether its neighboring layers are alike or different. The existence of such mixed sequences in "hexagonal" perovskite implies the appearance of $BO_6$ face-sharing octahedra (FSO).

Two types of hexagonal-cubic $AO_3$ stacking sequences can be distinguished for the *B*-site deficient "hexagonal" perovskite $A_nB_{n-1}O_{3n}$: $(hhc\ldots c)$ and $(hc\ldots c)$-type sequences (Fig. 1).

- In case of $(hhc\ldots c)$-type sequences (Fig. 1a), the vacancies are usually ordered between the *hh* layers resulting in a completely vacant octahedra layer located at the middle of FSO sequences (three octahedra layers thick). These structures can be described as a fully ordered stacking of blocks of $n-1$ octahedra layers (CSO blocks) separated by one vacant octahedra layer. Considering the resulting periodic shift of $1/3\langle 01\bar{1}0\rangle_H$ in the stacking of CSO blocks, this *B*-site deficient "hexagonal" perovskite will be further referred as "shifted" perovskite.

*Corresponding author. Fax: +33555457270.
*E-mail addresses:* trolliard@unilim.fr (G. Trolliard), dmercurio@unilim.fr (D. Mercurio).
[1] Also for correspondence.

0022-4596/$ - see front matter © 2003 Elsevier Inc. All rights reserved.
doi:10.1016/j.jssc.2003.10.024

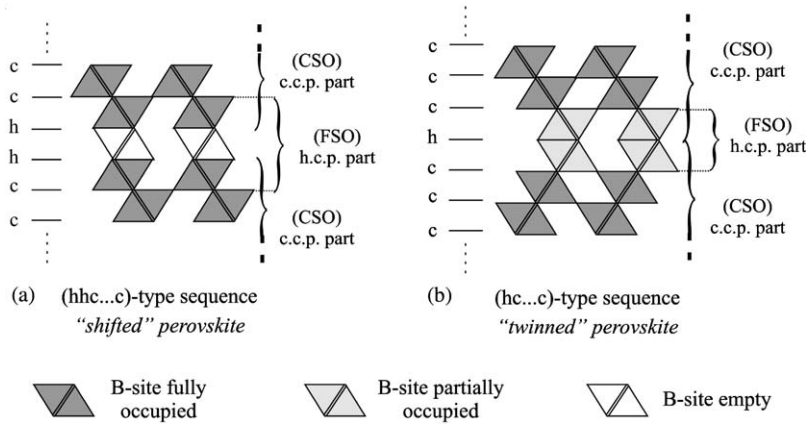


Fig. 1. Schematic representation of the two structural types of hexagonal perovskites encountered in the pseudo binary system $Ba_5Nb_4O_{15}$–$BaTiO_3$.

- In case of $(hc\ldots c)$-type sequences (Fig. 1b), the vacancies of *B*-sites does not result in the existence of a fully vacant octahedra layer but in a complex repartition of vacancies in FSO sequences of two octahedra layers thick. According to the intrinsic and periodically twinned character of the $AO_3$ layers stacking, this type of *B*-site deficient "hexagonal" perovskite will be further referred as "twinned" perovskite.

In the particular series $Ba_n(Nb,Ti)_{n-1}O_{3n}$ of the pseudo binary system $Ba_5Nb_4O_{15}$–$BaTiO_3$, "shifted" and "twinned" perovskites can be found depending on the value of the integer $n$. For $n = 5, 6, 7$ the "shifted" perovskite $Ba_5Nb_4O_{15}$ [3–5]—sequence 5H $(hhccc)$—and $Ba_6TiNb_4O_{18}$ [6]—sequence 18R $(hhcccc)_3$—$Ba_7Ti_2Nb_4O_{21}$ [7]—sequence 7H $(hhccccc)$, have been observed. For $n = 8$, the compound $Ba_8Ti_3Nb_4O_{24}$ [8] possesses a $(hccc)_2$ stacking sequence of $AO_3$ layers and appears to be the only stable "twinned" perovskite within this system. However, with a slightly different composition the compound $Ba_8B_{0.5}Ti_2Nb_{4.5}O_{24}$ ($n = 8$, and *B*: Lu, Yb…) displays "shift" type structure as shown by Mössner et al. [9] and thus exhibit a $(hhcc\ldots)$-type stacking of $AO_3$ layers. As these two compounds only differ by a cationic substitution on the *B*-site $(1Ti^{4+} \rightarrow 0.5B^{3+} + 0.5Nb^{5+})$, the role of the average size of the *B*-cation on the obtention of a "shift" type structure rather than a "twinned" type structure looks thus of importance.

To investigate further this influence of the average size of the *B*-cation on the structural type of such $n = 8$ compounds, we will first present a transmission electron microscopy (TEM) study of the solid solution $Ba_8Ti_{3-2x}Nb_{4+x}Lu_xO_{24}$ $(0 \leqslant x \leqslant 0.5)$ as a case study. In addition, a detailed discussion based on an accurate analysis of the literature of the so-called hexagonal perovskites with a general formula $A_nB_{n-1}O_{3n}$ $(n \geqslant 4)$, combined with a reexamination of the different terms of the $Ba_n(Nb,Ti)_{n-1}O_{3n}$ series will allow us to evidence the different factors which influence the stability of "shifted" or "twinned" type structures.

## 2. Structural background

As stated above two compounds, $Ba_8Ti_3Nb_4O_{24}$ [8] and $Ba_8Ti_2Nb_{4.5}Y_{0.5}O_{24}$ [9], which present similar stoichiometry and very close chemical composition crystallize respectively as "shifted" and "twinned" type structure.

The crystallographic characteristics of $Ba_8Ti_3Nb_4O_{24}$ are reported in Table 1. As illustrated in Fig. 2a, the crystal structure of $Ba_8Ti_3Nb_4O_{24}$ consists in a succession of CSO and FSO blocks with, respectively, a thickness of four $(m = 4)$ and two $(m = 2)$ $BO_6$ octahedra layers. A complete sequence along *c* corresponds to the succession of two twinned CSO blocks. The FSO sequences are formed by the two octahedra layers located on both side of the twinning plane. The main feature of the crystal structure is the distribution of cations and vacancies (□) on the *B*-sites. Three *B*-sites exist in the structure (Figs. 2a and b): $B(1)$ and $B(2)$ are located in the FSO sequences while $B(3)$ is in the middle of the CSO blocks. Refinement has evidenced a different cationic ordering for the $B(1)$ and $B(2)$ sites [8]. $B(1)$ roughly corresponds to $(1/2Nb + 1/2\square)$ and $B(2)$ to $(1/4Nb + 5/8Ti + 1/8\square)$. On the other hand, $B(3)$ is fully occupied, with a ratio Ti:Nb close to 1/2, i.e. $B(3) \sim (1/2Ti + 1/2Nb)$. The rate of vacancies for each *B*-site per formula unit is reported in Fig. 2b considering that the unit cell contains 3 formula units $Ba_8Ti_3Nb_4O_{24}$. Each $BO_6$ octahedra layer of the FSO thus contains $1 \times 1/6 + 2 \times 1/24 = 0.25$ vacancy per formula unit. So, the "twinned" type structure is characterized by the occurrence of 0.5 vacancy per formula unit in each FSO block (Fig. 2a) and consequently of 1

Table 1
Main structural characteristics of $Ba_8Nb_4Ti_3O_{24}$ [8] and $Ba_8Ti_2Nb_{4.5}Y_{0.5}O_{24}$ [9]

| Compound | Bravais system | Space group | Parameters (Å) |
|---|---|---|---|
| $Ba_8Nb_4Ti_3O_{24}$ ($n = 8$) | P | $P6_3/mcm$ | $a = 10.0677(1)$, $c = 18.9166(1)$ |
| $Ba_8Ti_2Nb_{4.5}Y_{0.5}O_{24}$ ($n = 8$) | R | $P\text{-}3m1$ | $a = 5.797(3)$, $c = 18.905(70)$ |

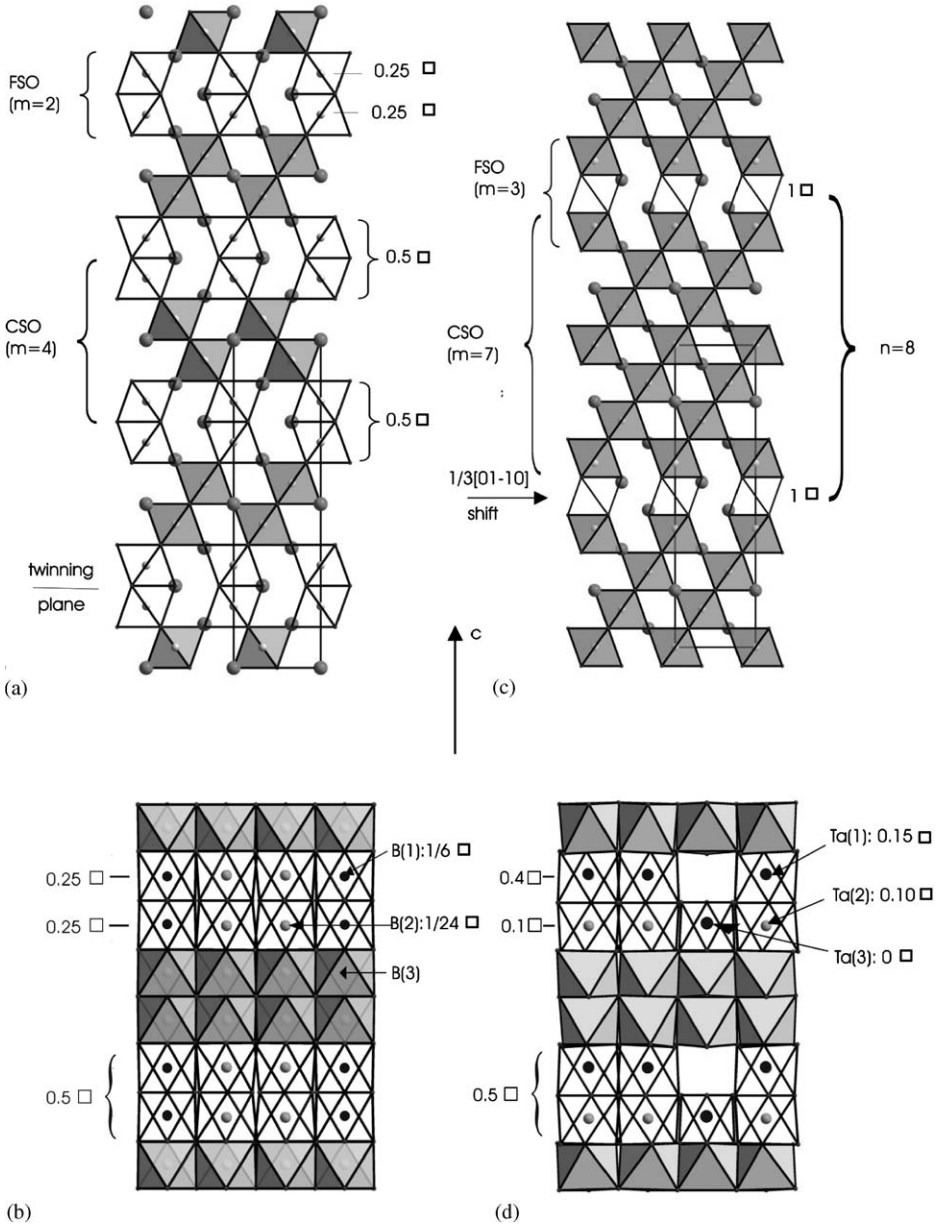


Fig. 2. Comparison of the vacancy distribution within octahedra layers in different compounds corresponding to the two structural types (shift and twin). (a) $Ba_8Ti_3Nb_4O_{24}$: structure as viewed along the $[1\bar{1}00]_H$ direction. (b) $Ba_8Ti_3Nb_4O_{24}$: structure as viewed along the $[2\bar{1}\bar{1}0]_H$ direction, i.e. the *a*-axis. (c) $Ba_8YbTi_2Nb_4O_{24}$: structure as viewed along the $[2\bar{1}\bar{1}0]_H$ direction, i.e. the *a*-axis. (d) $Ba_8Ta_6NiO_{24}$: structure as viewed along the $[2\bar{1}\bar{1}0]_H$ direction, i.e. the *a*-axis.

vacancy of *B*-cation by formula unit $Ba_8Ti_3Nb_4O_{24}$ giving rise to a $A_nB_{n-1}O_{3n}$ formula with $n = 8$.

The crystallographic parameters of $Ba_8Ti_2Nb_{4.5}Y_{0.5}O_{24}$ are reported in Table 1. As for $Ba_8Ti_3Nb_4O_{24}$, the crystal structure of $Ba_8Ti_2Nb_{4.5}Y_{0.5}O_{24}$ (Fig. 2c) consists in a succession of CSO and FSO blocks. However, they have different thickness compared to those of $Ba_8Ti_3Nb_4O_{24}$; the CSO (perovskite-like

Table 2
Starting chemical compositions of powders and results of TEM observations

| Composition | $\langle R_B \rangle$ | Homogeneity of the samples | Results of the TEM observations |
|---|---|---|---|
| $Ba_8Ti_2Nb_{4.5}Lu_{0.5}O_{24}$ | 0.646 Å | Pure preparation | Unique presence of $Ba_8Ti_2Nb_{4.5}Lu_{0.5}O_{24}$ "shift" structure type with $n = 8$ |
| $Ba_8Ti_{2.5}Nb_{4.25}Lu_{0.25}O_{24}$ | 0.635 Å | Heterogeneous sample | Mixed up of three phases: 80% of "shift" structure type with $n = 7$ and $n = 8$ +20% of additional "twin" structure type with $n = 8$ |
| $Ba_8Ti_{2.75}Nb_{4.125}Lu_{0.125}O_{24}$ | 0.630 Å | Homogenous preparation | ~100% of "twin" structure type with $n = 8$ |
| $Ba_8Ti_3Nb_4O_{24}$ | 0.625 Å | Pure preparation | Unique presence of $Ba_8Ti_3Nb_4O_{24}$ "twin" structure type with $n = 8$ |

blocks) and FSO blocks being here respectively of seven ($m = 7$) and three ($m = 3$) $BO_6$ octahedra thick. Two successive CSO blocks are shifted from one another by a $1/3\langle 01\bar{1}0 \rangle_H$ vector giving rise to the intermediate FSO sequence. This crystal structure is characterized by a full ordering of the *B*-cationic vacancies (□); they are strictly located in the central octahedra layer of the FSO. Thus, the $A_nB_{(n-1)}O_{3n}$ ($n = 8$) stoichiometry corresponds to the distribution of 1 vacancy per formula unit in each FSO blocks (Fig. 2c). So, in the "shifted" type structure all vacancies are concentrated in only one octahedra layer separated by identical CSO of $m = n - 1$ octahedra layer thick.

## 3. Experimental

All compounds were prepared as white powders by conventional solid-state synthesis using high-purity $Nb_2O_5$, $TiO_2$, $BaCO_3$ and $Lu_2O_3$. The starting materials were mixed in stoichiometric proportions in an agate mortar and fired at 1000°C for 10 h. Then, after crushing, all of the obtained powders were submitted to specific heating treatment, depending on the chemical composition.

A first set of experiments was performed in order to vary the average size of the *B*-cation, within the $n = 8$ $Ba_8Ti_{3-2x}Nb_{4+x}Lu_xO_{24}$ ($0 \leqslant x \leqslant 0.5$) solid solution. As indicated by the general formula, the substitution $2xTi^{4+} \rightarrow xLu^{3+} + xNb^{5+}$ were thus performed in samples with compositions ranging from $Ba_8Ti_3Nb_4O_{24}$ to $Ba_8Ti_2Nb_{4.5}Lu_{0.5}O_{24}$ (Table 2). All compounds were fired at 1400°C for 50 h. Compared to the other *B*-cations, the lutetium presents both a smaller valence (Ti: +IV, Nb: +V, Lu: +III) and a higher ionic radius ($r_{Ti^{4+}} = 0.605$ Å, $r_{Nb^{5+}} = 0.64$ Å, $r_{Lu^{3+}} = 0.86$ Å). The occurrence of lutetium does not influence the average valence of *B*-cations, but significantly increases the average ionic radius (Table 2). Therefore, the average *B* ionic radius $\langle R_B \rangle$ in $Ba_8Ti_3Nb_4O_{24}$ (0.625 Å) is smaller than in $Ba_8Lu_{0.5}Ti_2Nb_{4.5}O_{24}$ (0.646 Å).

In order to reinvestigate the $Ba_5Nb_4O_{15}$–$BaTiO_3$ system, the different terms of the $Ba_n(Ti,Nb)_{n-1}O_{3n}$ series ($n = 5, 6, 7, 8$) [3–8] were synthesized. The examination of Guinier patterns shows that after an annealing treatment of 50 h at 1300°C (case of $Ba_5Nb_4O_{15}$ [3–5]), and two runs of 50 h at 1400°C (case of $Ba_6TiNb_4O_{18}$ [6]), the powders samples are monophasic and correspond to the expected compounds. Powders of high purity were also obtained for $Ba_8Ti_3Nb_4O_{24}$ ($n = 8$) [8]. For the sample with $Ba_7Ti_2Nb_4O_{21}$ composition ($n = 7$), complex mixture is obtained. These results will be presented in detail and will be discussed below.

TEM observations were obtained using a JEOL 2010 microscope equipped with EDX facilities (Energy-dispersive X-ray analytical system), operating at 200 kV. The powder was first crushed in alcohol in an agate mortar, and then a drop of the suspension was deposited and dried on a copper grid coated with a thin film of amorphous carbon.

## 4. Results

Considering hexagonal perovskites with *c* as the stacking direction of the $AO_3$ layers, the most informative diffraction patterns and high-resolution images are those along the $\langle 1\bar{1}00 \rangle_H$ and $\langle 2\bar{1}\bar{1}0 \rangle_H$ zone axes for both "shift" and "twin" type structures (Fig. 2). The interpretation of SAED patterns and high-resolution images has been presented in details in previous papers [8,10–12].

### 4.1. Reinvestigation of the $Ba_n(NB,Ti)_{n-1}O_{3n}$ series : n=5,6,7,8

As previously noted in the experimental session, the compounds with $n = 5, 6, 8$ were easily obtained and in each cases, powders with rather high purity were synthesized. All high-resolution images as well as SAED patterns obtained of the compounds $n = 5, 6, 8$ attest that crystals are well ordered and free of stacking faults, as previously reported in the literature [8,11]. On the contrary, the sample of $Ba_7Ti_2Nb_4O_{21}$ ($n = 7$) composition always display complex mixture that evolves depending on heating treatment. After the conventional annealing treatment of 50 h at 1300°C, used to

synthesize the other terms ($n = 5, 6, 8$), the samples of $Ba_7Ti_2Nb_4O_{21}$ ($n = 7$) always exhibits three phases:

- $Ba_6TiNb_4O_{18}$ ($n = 6$) and $Ba_7Ti_2Nb_4O_{21}$ ($n = 7$), with a "shift" type structure,
- $Ba_8Ti_3Nb_4O_{24}$ ($n = 8$) with a "twin" type structure.

Moreover, one must notice that the $n = 7$ term (Fig. 3) is very often composed of disordered crystals showing an intergrowth of $n = 7$ and 6 sequences with a "shift" type structure giving rise to diffusion streaks along the $c^*$ direction of the SAED patterns. Longer annealing time (200 h at 1350°C, as predicted by Mössner et al. [9]) or at more elevated temperature (50 h at 1400°C) always failed to grow $Ba_7Ti_2Nb_4O_{21}$ and gave biphasic samples composed of $Ba_6TiNb_4O_{18}$ ($n = 6$ with a "shift" type structure) and $Ba_8Ti_3Nb_4O_{24}$ ($n = 8$ with a "twin" type structure), testifying that $Ba_7Ti_2Nb_4O_{21}$ decomposes during heating treatments.

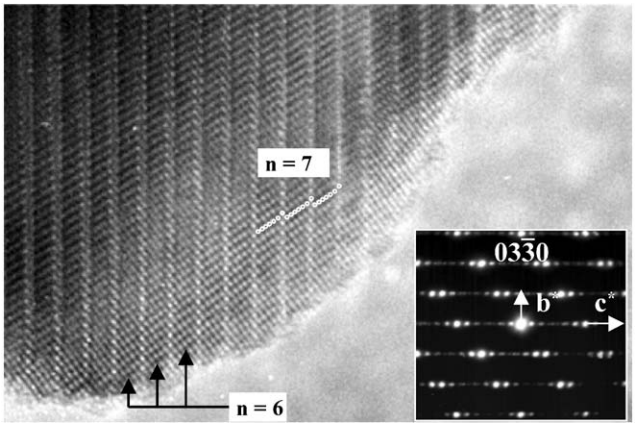


Fig. 3. HREM images obtained on a crystal of the powder sample with $Ba_7Ti_2Nb_4O_{21}$ composition. $n = 7$ sequences within the perovskite blocks are shown by the alignment of the white circles but they coexist with $n = 6$ perovskite blocks. The SAED patterns presents diffusion streaks along the $c^*$ direction in agreement with this stacking disorder.

### 4.2. Study of the solid solution $Ba_8Ti_{3-2x}Nb_{4+x}Lu_xO_{24}$ ($0 \leqslant x \leqslant 0.5$) with $n = 8$

The main results obtained on the different samples of the solid solution are reported in Table 2.

TEM observations carried out on $Ba_8Ti_2Nb_{4.5}Lu_{0.5}O_{24}$ ($x = 0.5$ and $\langle R_B \rangle = 0.646$ Å) show crystallites that present "shift" type structure with $n = 8$ (Fig. 4). SAED patterns show very sharp diffraction spots attesting that the crystals are well ordered, without any defects. Numerous observations performed in order to get statistical information suggest that the powder is monophasic. Chemical analyses confirm the presence of lutetium within crystals (Fig. 4).

At the opposite, the samples with composition $Ba_8Ti_3Nb_4O_{24}$ ($x = 0$, $\langle R_B \rangle = 0.625$ Å) and $Ba_8Ti_{2.75}Nb_{4.125}Lu_{0.125}O_{24}$, ($x = 0.125$ : $\langle R_B \rangle = 0.630$ Å) are solely composed of micro twinned crystals (Fig. 5). Again, the powders can be considered as monophasic.

For the intermediate composition $Ba_8Ti_{2.5}Nb_{4.25}Lu_{0.25}O_{24}$ ($x = 0.25$ : $\langle R_B \rangle = 0.635$ Å) both "shift" and "twin" type structures are observed (Fig. 6). The respective amount of the two structural types is estimated as 80/20 on the basis of TEM observations (Table 2). The occurrence of these two structural types in the same sample can be connected with a partial phase separation of the nominal "twin" type composition into the two more stable "shift" and "twin" phases of the system. However, the presence of a "shift" type structure type can also be relevant to inhomogeneous repartition of Lu in the crystals.

In summary, when the ionic radius of the *B*-cations is high (case of $Ba_8Ti_2Nb_{4.5}Lu_{0.5}O_{24}$), the "shift" structure type prevails while when the ionic radius of the

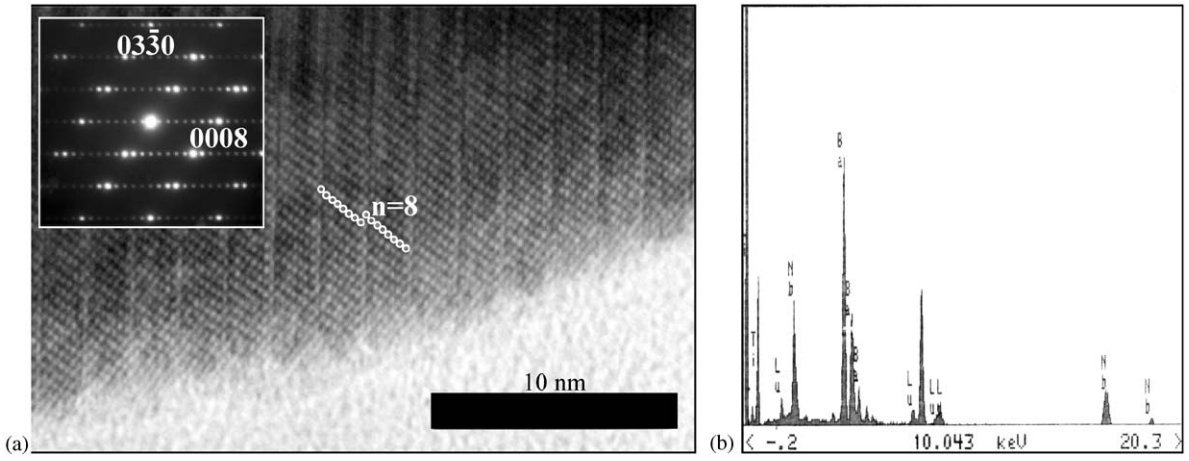


Fig. 4. TEM observations performed on $Ba_8Ti_2Nb_{4.5}Lu_{0.5}O_{24}$ ($\langle R_B \rangle = 0.646$ Å). (a) HREM image with $[2\bar{1}\bar{1}0]_H$ zone axis and related SAED patterns. (b) XRD analysis of the crystal showing the presence of lutetium.

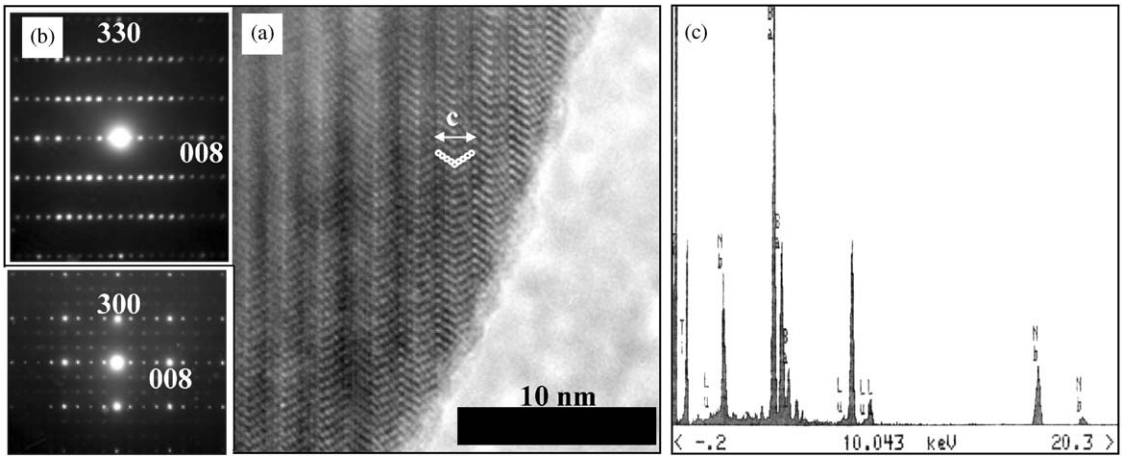


Fig. 5. TEM observations obtained on $Ba_8Ti_{2.75}Nb_{4.125}Lu_{0.125}O_{24}$ ($\langle R_B \rangle = 0.630$ Å). (a) HREM image obtained on a crystal viewed along the $[1\bar{1}00]_H$ zone axis. (b) Two SAED patterns of this crystal orientated along the $[1\bar{1}00]_H$ and $[2\bar{1}\bar{1}0]_H$ zone axis. (c) XRD analysis of the crystal showing the presence of lutetium.

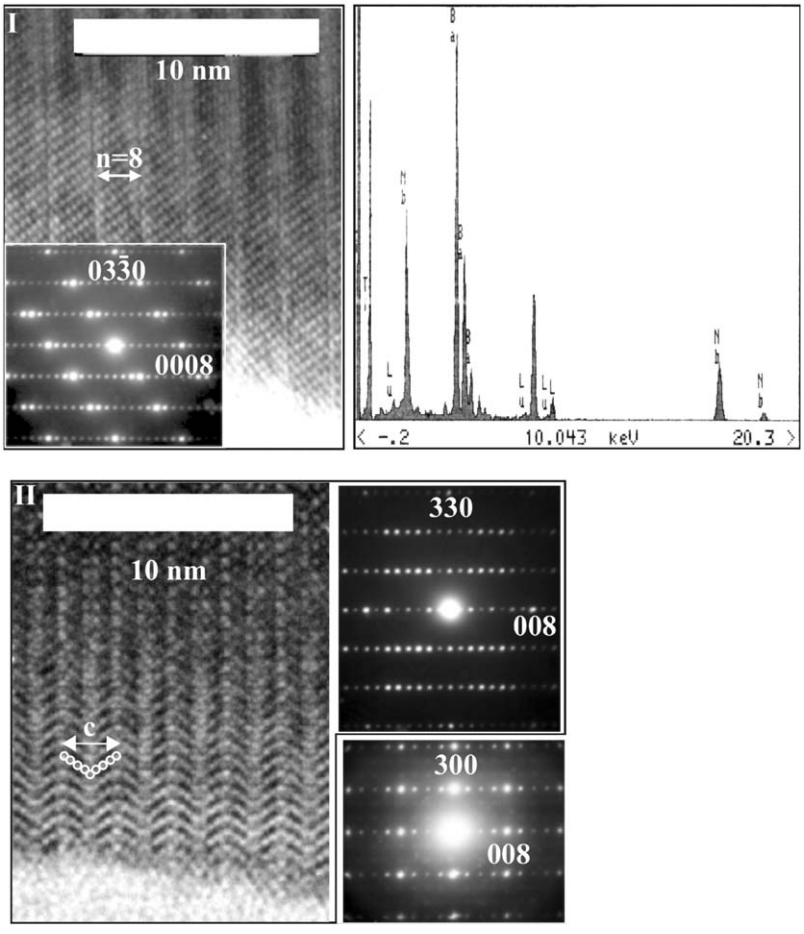


Fig. 6. TEM observations performed on a powder with a composition $Ba_8Ti_{2.5}Nb_{4.25}Lu_{0.25}O_{24}$ ($\langle R_B \rangle = 0.635$ Å) showing the coexistence of different structural terms belonging to both twin and shift types. I: HREM and related SAED patterns and XRD analysis of a compound of $n = 8$ with a shift type structure. II: HREM of a compound of $n = 8$ showing a twin type structure and two SAED patterns obtained on the same crystal with $[1\bar{1}00]_H$ and $[2\bar{1}\bar{1}0]_H$ zone axis.

*B*-cations is low (case of $Ba_8Ti_3Nb_4O_{24}$), only the "twin" type structure is observed. The heterogeneous character of the intermediate composition $Ba_8Ti_{2.5}Nb_{4.25}Lu_{0.25}O_{24}$ suggests that neither "twin" nor "shift" type structure is preferably formed but a mixing of both of them with different compositions.

## 5. Discussion

The results obtained during this study have confirmed the influence of the average size of the *B*-cation on the stability of the structural type, i.e. "twin" or "shift" modes, for a given size of *A*-cation. However, in order to discuss of the stability of "twin" and "shift" structure types in various chemical systems, a comprehensive discussion imposes to consider the influence of the *A*-cation as well. The Goldschmidt tolerance factor $t = (R_{A^{x+}} + R_{O^{2-}})/\sqrt{2}(R_{B^{y+}} + R_{O^{2-}})$, which is classically used to state upon the stability of pure or related type perovskite structures, allows to consider the relative size of *A*- and *B*-cations. Structural characteristics of principal phases $A_nB_{n-1}O_{3n}(n \geqslant 4)$ reported in the literature, which crystallize with an hexagonal cation-deficient-perovskite related structure, are provided in Table 3. These compounds can either belong to a series within a single system (*A* part of the Table 3) or as isolated terms (*B* part of Table 3) grouped according to their value of *n*. Stability domains of "twin" and "shift" structure types as a function of *n* and *t* are shown in Fig. 7, which represents a compilation of the data presented in Table 3. The examination of these data leads to the following remarks:

- whatever the value of *t*, the compound with low *n* ($n = 4, 5, 6$) always display "shift" type structure, which is thus stabilized in a wide range of *t* values, typically $0.97 \leqslant t \leqslant 1.05$ (domain I in Fig. 7).
- "twin" structures are seldom observed and always correspond to compounds with high values of *n* ($n > 7$) and *t* ($t > 1.05$) (domain II in Fig. 7). To our knowledge for the whole of $A_nB_{n-1}O_{3n}$ ($n \geqslant 4$) phases the "twin" structure type has been stabilized only for $n = 8$. $Ba_{10}Ta_{7.04}Ti_{1.2}O_{30}$ which presents also a "twin" structure with $n = 10$ corresponds to another stoichiometry, i.e. $\sim A_nB_{n-2}O_{3n}$ [22].

The remarkable stability of the "shift" type structure (Fig. 7) for a large range of *t* can be explained by the occurrence of a regular "CsCl-type" cation sub-lattice, which is a structural characteristic of these perovskites. In a previous paper [10] we have already shown that the shift of a $1/3\langle 01\bar{1}0\rangle_H$ vector between two successive CSO perovskite blocks (Fig. 1) coupled to the cationic relaxation effect along Oz, leads to the preservation of a body-centered cubic (bcc) cationic sub-lattice.

In the "shift" type structure, the *B*-vacancy by unit formula $A_nB_{n-1}O_{3n}$ ($n > 4$) leads to a fully vacant octahedra layer located between the CSO blocks (Fig. 2a). These vacancies are periodically ordered each *n* octahedra layers along the *c*-axis. When n increases this spacing becomes too important and then the "shift" structure turns to the "twin" structure (Fig. 1a). In the "twin" type structure, the distance between two *B*-vacancies strongly decreases (Fig 2b) leading to a more homogeneous distribution of defects within the structure. Indeed, 0.5 *B*-vacancies are distributed within the two octahedra layers of the FSO sequences (0.25 in each one), the latter being spaced solely by $n/2$ octahedra layers.

The "twin" type structure, which requires a simultaneous occupation of the two face-sharing octahedra

Table 3
Different shift and twin compounds encountered in the literature with $AB_{(n-1)}O_{3n}$ general formula

| Ref. | Compound named | *n* value | *t* value | Structural type |
|---|---|---|---|---|
| **A** | | | | |
| [12–14] | $La_4Ti_3O_{12}$ | 4 | 0.9734 | Shift |
| [10,15] | $BaLa_4Ti_4O_{15}$ | 5 | 0.991 | Shift |
| [10,16] | $Ba_2La_4Ti_5O_{18}$ | 6 | 1.0028 | Shift |
| [12–14] | $La_4Ti_3O_{12}$ | 4 | 0.9734 | Shift |
| [12,17] | $La_5Ti_4O_{15}$ | 5 | 0.9734 | Shift |
| [12,17] | $La_6Ti_5O_{18}$ | 6 | 0.9734 | Shift |
| [3–5] | $Ba_5Nb_4O_{15}$ | 5 | 1.0433 | Shift |
| [6] | $Ba_6TiNb_4O_{18}$ | 6 | 1.0469 | Shift |
| [This study, 7] | $Ba_7Ti_2Nb_4O_{21}$ | 7 | 1.0493 | Decomposition |
| [8] | $Ba_8Ti_3Nb_4O_{24}$ | 8 | 1.0511 | Twin |
| **B** | | | | |
| [12–14] | $La_4Ti_3O_{12}$ | 4 | 0.9734 | Shift |
| [19] | $Ba_3LaNb_3O_{12}$ | | 1.0433 | Shift |
| [18] | $Ba_4Nb_2WO_{12}$ | | 1.0502 | Shift |
| [19] | $CaLa_4Ti_4O_{15}$ | 5 | 0.972 | Shift |
| [19] | $SrLa_4Ti_4O_{15}$ | | 0.979 | Shift |
| [19] | $BaLa_4Ti_4O_{15}$ | | 0.991 | Shift |
| [20] | $CaLa_4Ti_3RuO_{15}$ | | 0.9701 | Shift |
| [20] | $SrLa_4Ti_3RuO_{15}$ | | 0.9772 | Shift |
| [20] | $BaLa_4Ti_3RuO_{15}$ | | 0.9892 | Shift |
| [17] | $La_5Ti_4O_{15}$ | | 0.9734 | Shift |
| [12,17] | $La_6Ti_5O_{18}$ | 6 | 0.9734 | Shift |
| [19] | $Ca_2La_4Ti_5O_{18}$ | | 0.971 | Shift |
| [21] | $Ba_5SrTa_4ZrO_{18}$ | | 1.0255 | Shift |
| [21] | $Ba_6Ta_4ZrO_{18}$ | | 1.0352 | Shift |
| [9] | $Ba_7Sc_{0.5}Nb_{4.5}TiO_{21}$ | 7 | 1.0418 | Shift |
| [9] | $Ba_7In_{0.5}Nb_{4.5}TiO_{21}$ | | 1.0395 | Shift |
| [9] | $Ba_7Y_{0.5}Nb_{4.5}TiO_{21}$ | | 1.0303 | Shift |
| [9] | $Ba_7Tm_{0.5}Nb_{4.5}TiO_{21}$ | | 1.0299 | Shift |
| [This study, 7] | $Ba_7Ti_2Nb_4O_{21}$ | | 1.0493 | Shift |
| [21] | $Ba_5Sr_2Ta_4Zr_2O_{21}$ | | 1.0132 | Shift |
| [21] | $Ba_7Ta_4Zr_2O_{21}$ | | 1.0299 | Shift |
| [This study] | $Ba_8Ti_2Nb_{4.5}Lu_{0.5}O_{24}$ | 8 | 1.0404 | Shift |
| [This study] | $Ba_8Ti_{2.5}Nb_{4.25}Lu_{0.25}O_{24}$ | | 1.0457 | Mixed |
| [This study] | $Ba_8Ti_{2.75}Nb_{4.125}Lu_{0.125}O_{24}$ | | 1.0484 | Twin |
| [This study, 8] | $Ba_8Ti_3Nb_4O_{24}$ | | 1.0511 | Twin |
| [21] | $Ba_5Sr_3Ta_4Zr_3O_{24}$ | | 1.0044 | Shift |
| [22] | $Ba_8Ti_3Ta_4O_{24}$ | | 1.0433 | Twin |
| [23] | $Ba_8Ta_6NiO_{24}$ | | 1.0397 | Twin |

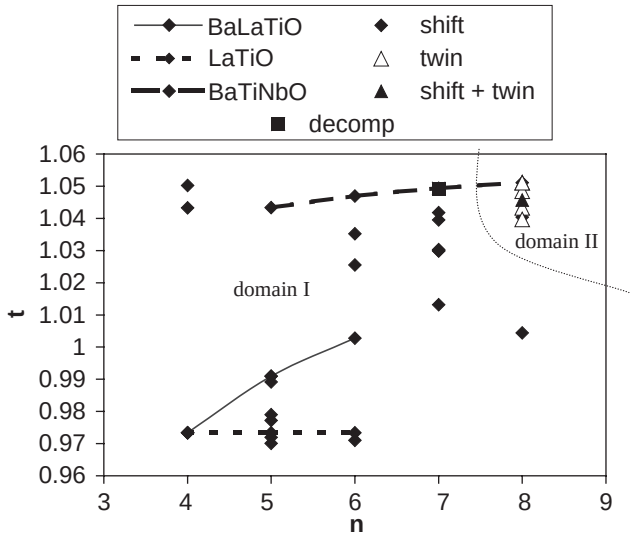


Fig. 7. $t-n$ Correlations for $A_nB_{n-1}O_{3n}(n\geqslant 4)$ "shift", "twin" type structures (established from Table 3). — $(Ba,La)_nTi_{n-1}O_{3n}$ series ($n=4,5$ and 6); --- $La_nTi_{n-1}O_{3n}$ series ($n=4,5$ and 6); –– $Ba_n(Ti, Nb)_{n-1}O_{3n}$ series ($n=5,6,7$ and 8).

(FSO), can be stabilized only for the large values of $t$. In such a case, the resulting expansion of the three-dimensional lattice of $BO_6$ octahedra, which is correlated to an increasing volume of each $BO_6$ octahedra, leads to elongated $B-B$ cationic distances favoring the simultaneous occupation of the two $B$-sites situated on each side of the twinning plane. This fact will be all the more enhanced by small size and low charge of the $B$-cations. On contrary, when the value of $t$ is too small, the distance between FSO centers became too short to allow the simultaneous occupation of these two $B$-sites and the twin type structure is no longer stable.

In this study, the $Ba_8Ti_3Nb_4O_{24}$ compound shows "twin" type structure in agreement with the large value of $t$ ($t=1.05$). In addition, the specific $B$-cationic ordering evidenced in this phase [8] avoids strong $B-B$ interactions ($Nb^{5+}$–$Nb^{5+}$ pairs). This cationic ordering in FSO seems to be a specific characteristic of the "twin" mode [23], which could enhance the stability domain of the "twin" type structure.

In this phase the progressive substitution $2xTi^{4+}\rightarrow xNb^{+5}+xLu^{3+}$ leads to increase the average size $\langle R_B\rangle$ of the $B$-cation and correlatively to decrease $t$ (Table 3). As a result, in $Ba_8Ti_{3-2x}Nb_{4+x}Lu_xO_{24}$ ($0\leqslant x\leqslant 0.5$) solid solution, when $x$ increases, the structure logically changes from a "twin" type structure to a "shift" type structure.

$Ba_8Ta_6NiO_{24}$ [23] is therefore a peculiar case because this phase presents a "twin" type structure whereas, for the same value of $t=1.04$, $Ba_8Ti_2Nb_{4.5}Lu_{0.5}O_{24}$ crystallizes with a "shift" type structure. In this compound, the specific cationic ordering observed in FSO (no $Ta^{5+}$–$Ta^{5+}$ pairs and only existence of $Ni^{2+}$–$Ta^{5+}$ pairs affected by a low average charge) facilitates the establishment of the "twin" type structure.

To our knowledge, the "twin" type structure always corresponds to phases with $n=8$ (Table 3). $Ba_{10}Ti_{1.2}Ta_{7.04}O_{30}$ [22] is also a peculiar case since it presents a specific stoichiometry close to $A_nB_{n-2}O_{3n}$. So, one vacancy (and not half: see Fig. 2a) is randomly distributed in FSO every five octahedra layers. Owing to this specific amount of vacancies, $B-B$ couple do not exist in the FSO and thus the stability of the "twin" type structure for $n=10$ is privileged.

For $Ba_7Ti_2Nb_4O_{21}$ ($n=7$), the present study shows that this compound behave as metastable phase. The value of the theoretical Goldschmidt factor $t=1.05$, superior to those of homologous phases with $n=7$ (Table 3), can enhance the stability of the "twin" type structure. Nevertheless, according to the periodicity of vacancies each $n/2$ octahedra layers, the "twin" type structure cannot exist in cation-deficient-perovskite related $A_nB_{n-1}O_{3n}$ for odd values of $n$. As a result, for this composition a phase separation occurs which gives rise to the two nearest stable phases, i.e. $Ba_6TiNb_4O_{18}$ ("shift" type structure with $n=6$) and $Ba_8Ti_3Nb_4O_{24}$ ("twin" type structure with $n=8$).

## 6. Conclusions

In the $B$-cation deficient perovskite-related compounds $A_nB_{n-1}O_{3n}$, the non-stoichiometry is in any cases closely associated with the distribution of planar defects: shift planes or twin boundaries. The respective stability of both "shift" and "twin" type structures seems to rely on a competition between several parameters:

- In the "shift" type structure the particular stability of the cationic sub-lattice is in competition with the establishment of a long-range ordering of vacancies, every $n$ octahedra layers along the $c$-axis, which is more and more difficult to obtain as n increases.
- The stability of the "twin" type structure is surely due to the drastic decrease of the periodicity of vacancies along the $c$-axis (every $n/2$ octahedra layers) but needs a very expanded three dimensional $BO_6$ octahedra sub-lattice (high value of $t$). This structural type is also favored by a specific ordering of $B$-cations in the FSO blocks, which is necessary to avoid the strong repulsive interactions between $B$-cations. The distribution of vacancies implies that n is even.

## References

[1] Jagodzinski, Acta Crystallogr. 4 (2) (1949) 201.
[2] D. Pandey, P. Krishna, Layer stacking in closed packed structures, in: Hahn, T. (Ed.), International Tables for Crystallography, Vol. C, Kluwer Academic Publishers, Dordrecht, 1989.

[3] N. Massa, S. Pagola, R. Carbonio, Phys. Rev. B 53 (16) (1996) 8148.
[4] L. Hutchinson, A.J. Jacobson, J. Solid State Chem. 20 (1977) 417.
[5] S. Pagola, G. Polla, G. Leyva, et al., Mater. Sci. Forum 228–231 (1996) 819.
[6] H.C. Van Duivenboden, H.W. Zandbergen, D.J.W. Ijdo, Acta Crystallogr. C 42 (1986) 266.
[7] B. Mossner, S. Kemmler-Sack, J. Less-Common Metals 120 (1986) 287.
[8] N. Teneze, P. Boullay, V. Petricek, G. Trolliard, D. Mercurio, Solid State Sci. 4 (2002) 1129.
[9] B. Mossner, S. Kemmler-Sack, J. Less-Common Metals 120 (1986) 203.
[10] G. Trolliard, N. Harre, D. Mercurio, B. Frit, J. Solid State Chem. 145 (1999) 678.
[11] G. Trolliard, N. Teneze, Ph. Boullay, M. Manier, D. Mercurio, J. Solid State Chem. 173 (2003) 91.
[12] G. Van Tendeloo, S. Amelincks, R. Bontchev, J. Darriet, F. Weill, J. Solid State Chem. 108 (1994) 314.
[13] N.F. Fedorov, O.V. Mel'nikova, V.A. Saltikova, V.M. Chistykova, Russ. J. Inorg. Chem. 24 (5) (1979) 649.
[14] N. Teneze, D. Mercurio, G. Trolliard, B. Frit, Mater. Res. Bull. 35 (10) (2000) 1604.
[15] N. Harre, D. Mercurio, G. Trolliard, B. Frit, Mater. Res. Bull. 33 (10) (1998) 1537.
[16] N. Harre, D. Mercurio, G. Trolliard, B. Frit, Eur. J. Solid State Chem. 35 (1998) 77.
[17] R. Bontchev, B. Darriet, J. Darriet, F. Weill, G. Van Tendeloo, S. Amelincks, Eur. J. Solid State Chem. 30 (5) (1993) 521.
[18] H.J. Von Rother, S. Kemmler-Sack, U. Treiber, W.R. Cyris, Z. Anorg. Allg. Chem. 466 (1980) 131.
[19] M. German, L.M. Kovba, Russ. J. Inorg. Chem. 28 (9) (1980) 2377.
[20] R. Bontchev, F. Weill, J. Darriet, Mater. Res. Bull. 27 (1992) 931.
[21] A.M. Abakumov, R.V. Shpanchenko, E.V. Antipov, O.I. Lebedev, G. Van Tendeloo, S. Amelincks, J. Solid State Chem. 141 (1998) 492.
[22] R.V. Shpanchenko, L. Nistor, G. Van Tendeloo, J. Van Landuyt, S. Amelincks, A.M. Abakumov, E.V. Antipov, L.M. Kovba, J. Solid State Chem. 114 (1995) 560.
[23] A.M. Abakumov, G. Van Tendeloo, A.A. Scheglov, R.V. Shpanchenko, E.V. Antipov, J. Solid State Chem. 125 (1996) 102.